Vibrational spectroscopy of phase transitions in leonite-type minerals

BIRGIT HERTWECK and EUGEN LIBOWITZKY*

Institut für Mineralogie und Kristallographie, Universität Wien – Geozentrum, Althanstraße 14, A-1090 Wien, Austria
* Corresponding author, e-mail: eugen.libowitzky@univie.ac.at

Abstract: Infrared (IR) and Raman spectra of leonite-type minerals, $K_2Me(SO_4)_2 \cdot 4H_2O$ (Me = Mg, Mn, Fe), confirm a succession of structural phase transitions between 277 and 120 K. Because the orientation and dynamic behaviour of the sulphate tetrahedra undergo the most conspicuous changes during these transitions, transmission IR and Raman spectra were recorded for the SO_4 bending and stretching modes from 660 to 1230 cm^{-1} (IR) and 350 to 1250 cm^{-1} (Raman), in a temperature range between 80 K and room temperature.

At low temperature the leonite-type minerals show an order-disorder phase transition due to the freezing of the dynamic sulphate disorder. These phase transitions are characterised by non-linear shifts of the peak positions as a function of temperature in IR and Raman spectra. Evaluation of the peak widths of the sulphate modes in the IR and Raman spectra by autocorrelation analysis show non-linear decreases of the width parameters, confirming a tricritical ordering process according to the Landau order parameter. With decreasing temperature the crystal structures of the Mg- and Mn-endmembers switch to another ordered phase. These structural changes are accompanied by the sudden appearance of additional sulphate stretching and bending modes and by discontinuities of the peak shifts in IR and Raman spectra, indicating a first order phase transition.

Key-words: leonite, autocorrelation analysis, IR/Raman spectroscopy, phase transitions, tricritical.

Introduction

The structure of leonite-type minerals and compounds, $K_2Me(SO_4)_2 \cdot 4H_2O$ (Me = Mg, Mn, Fe), space group $C2/m$, consists of two crystallographically different MeO_6 octahedra, assembled in the form of $Me[(H_2O)_4(SO_4)_2]^{2-}$ units, with the sulphate groups in *trans* conformation and the S–Me–S axes oriented nearly parallel to [100]. These units are interconnected by potassium cations and by hydrogen bonds of the H_2O molecules. At room temperature the sulphate groups of one $Me[(H_2O)_4(SO_4)_2]^{2-}$ unit are disordered (Srikanta *et al.*, 1968).

These dynamically disordered sulphate tetrahedra freeze at low temperatures to an ordered structure with space group $I2/a$ in the Mg- and Mn-endmembers (Hertweck *et al.*, 2001). Upon further cooling, the ordered arrangement in leonite and "Mn-leonite"[1] switches to another modification (space group $P2_1/a$) with different sulphate ordering scheme. In mereiterite, the Fe-endmember, only one transition from the dynamically disordered $C2/m$ structure to the ordered $P2_1/a$ structure is observed.

During the phase transitions the distortion of the structure leads to changes of the space group symmetry and to a distortion of the optical indicatrix. Analyses of single-crystal

X-ray reflection intensities and of the excess birefringence as a function of temperature (Hertweck *et al.*, 2002) indicate that according to Landau theory the $C2/m \leftrightarrow I2/a$ ($P2_1/a$ for mereiterite) order-disorder transitions are tricritical. The displacive $I2/a \leftrightarrow P2_1/a$ phase transition of leonite and "Mn-leonite" is of first order type. The information obtained from a combined approach using single-crystal X-ray diffraction, crystal optics, and calorimetric data (Hertweck *et al.*, 2001, 2002) is supported by infrared (IR) and Raman spectroscopy in the present study.

Experimental

For Raman spectroscopic measurements synthetic single-crystals of leonite-type compounds were ground and polished manually with Al_2O_3 grinding films on one side of the slabs to ensure proper alignment and heat transfer on the heating/cooling stage. Oriented measurements were performed on the single-crystals in backscattering geometry a(c b/c)a', with the incident beam parallel to *a* and the polarisation of the incident laser parallel to *c*.

A notch filter-based micro-Raman system Renishaw RM 1000 equipped with a Leica DMLM series microscope and with a Si-based, Peltier-cooled charge-coupled device (CCD) detector was used for laser-Raman micro-spectroscopy. Spectra were excited with the 632.8 nm line of a He-

---

[1] "Mn-leonite" is not a name for a mineral, but is used in agreement with previous literature, *i.e.* Schneider (1961).

Ne laser. A Leica 50 × long working distance objective (numerical aperture 0.55) was used for measurements in non-confocal mode. For the measurements between 78 K (leonite), 140 K ("Mn-leonite"), 160 K (mereiterite), respectively, and room temperature a LINKAM THMS 600 heating/cooling stage with an absolute temperature accuracy of ±1 K was used. The temperature was controlled with a LINKAM TP93 heating/cooling device with a LINKAM LNP liquid nitrogen supply. During data acquisition the temperatures were kept constant to ±0.2 K.

Measurements were done in backscattering geometry in the sulphate tetrahedral stretching and bending range (350-1250 cm^{-1}) in so-called "continuous extended scan" data collection mode (*cf.* Nasdala & Massonne, 2000). The Raman system was equipped with a grating with 1200 grooves per millimetre, resulting in a wavenumber accuracy better than 1 cm^{-1} and a spectral resolution of ~5 cm^{-1}. The system was calibrated using the 520 cm^{-1} line of a Si standard. Because only relative changes of the band widths are investigated, mathematical correction of the full width at half maximum (FWHM) values for the apparatus function (Irmer, 1985; Verma *et al.*, 1995) was not applied. Depending on the signal intensity, 3-6 accumulations with 30 to 60 seconds per "spectral window" (*i.e.*, exposure time of the detector) were measured, which resulted in overall analytical times of 15-20 minutes per single analysis. Computational control and graphical presentation of the measurements were done with Grams/32 software (Galactic Ind. Corp.). FWHMs and peak centres of single bands were determined by fits of combined Gaussian/Lorentzian functions using Peak Fit software (Jandel Scientific).

Strong absorption of the leonite-type compounds in the range of the IR bands required the preparation of extremely thin single-crystal slabs. However, because of the brittle quality of the samples these grinding attempts were not successful. Thus, the samples were ground to powder and pressed to KBr pellets with a diameter of 13 mm and a sample/KBr ratio of about 0.005.

The unpolarised transmission IR spectra were recorded from 660 cm^{-1} to 4000 cm^{-1} on a Perkin-Elmer FTIR microscope, attached to a Perkin-Elmer 1760X FTIR spectrometer. For the measurements between 80 K (leonite), 90 K ("Mn-leonite"), 140 K (mereiterite), respectively, and room temperature the same LINKAM THMS 600 heating/cooling stage as described above was used. In case of IR spectroscopy the stage was equipped with BaF$_2$ windows. The microscope was equipped with 6x/0.60 N.A. mirror lenses (Cassegrains), and a liquid nitrogen cooled wide-range MCT detector.

Background and sample spectra were averaged from 64 single scans each with a nominal resolution of 4 cm^{-1}. Background corrections and determination of band centres were done with Spectrum software (Perkin-Elmer).

Results and discussion

Because the orientation and dynamic behaviour of the sulphate tetrahedra undergo the most conspicuous changes within the structural phase transitions, Raman and FTIR ab-
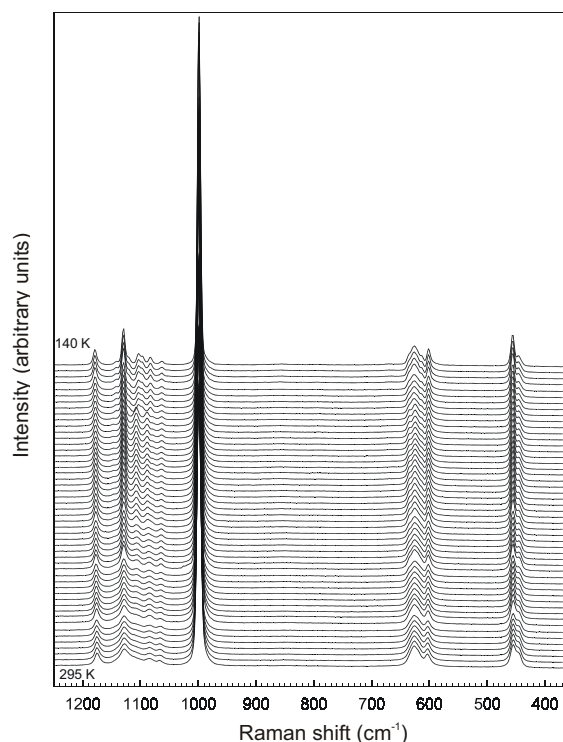

Fig. 1. Raman spectra of the vibrational modes of the sulphate tetrahedra in "Mn-leonite" in the temperature range between 295 and 140 K. Spectra are measured in temperature steps of 5 K between 295 and 215 K, of 2 K between 215 and 205 K, of 1 K between 205 and 200 K, of 2 K between 200 and 186 K, of 3 K between 186 and 180 K, of 2 K between 180 and 170 K, of 1 K between 170 and 166 K, of 3 K between 166 and 160 K, and of 5 K between 160 and 140 K. The spectra are displayed normalised in peak height with an offset of 5000 counts.

sorption spectra were recorded in the region of the tetrahedral bending and stretching modes. As the sulphate tetrahedra are surrounded by hydrogen bonds which influence the cooperative arrangement of tetrahedra during the phase transitions, FTIR absorption spectra were also acquired in the region of the H$_2$O stretching modes.

According to the different phase stability ranges of the three compounds, the Raman and FTIR absorption spectra were recorded in different, appropriate temperature ranges, as listed in the Fig. captions. To investigate pre-and post-transitional effects on the absorption, the spectra were acquired in variable temperature steps around the phase transition temperatures.

Raman spectroscopy

An example of the Raman spectra of "Mn-leonite" from 350 to 1250 cm^{-1} is given in Fig. 1. In the region from 1030 to 1200 cm^{-1} the ν_3 (antisymmetric stretching) modes, around 1000 cm^{-1} the ν_1 (symmetric stretching) mode, from 580 to 670 cm^{-1} the ν_4 (antisymmetric bending) modes, and from 430 to 470 cm^{-1} the ν_2 (symmetric bending) modes of the sulphate tetrahedra are observed (Nakamoto, 1997). Details
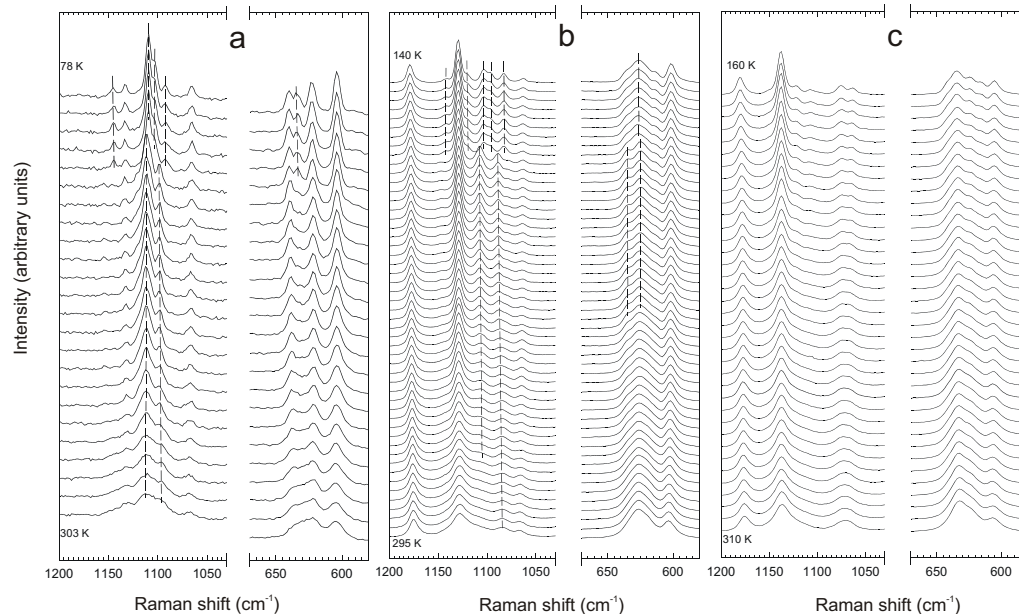
Fig. 2. Raman spectra of the sulphate ν_3 and ν_4 modes in leonite-type compounds. Vertical lines (as a guide for the eye) indicate the appearance or disappearance, respectively, of vibrational modes at the $I2/a \leftrightarrow P2_1/a$ phase transitions for leonite and "Mn-leonite". **(a)** Raman spectra of leonite in the temperature range between 303 and 78 K measured in temperature steps of 10 K between 303 and 83 K. Phase transitions at 269 and 120 K. **(b)** Raman spectra of "Mn-leonite" in the temperature range between 295 and 140 K. Phase transitions at 205 and 169 K. Temperature intervals as indicated in Fig. 1. **(c)** Raman spectra of mereiterite in the temperature range between 310 and 160 K measured in temperature steps of 5 K (310–285 K), of 2 K (285–279 K), of 1 K (279–270 K), of 2 K (270–260 K), of 5 K (260–220 K), and of 10 K (220–160 K). Phase transition at 277 K. The intensity-normalised spectra are displayed with an offset of 5000 counts.
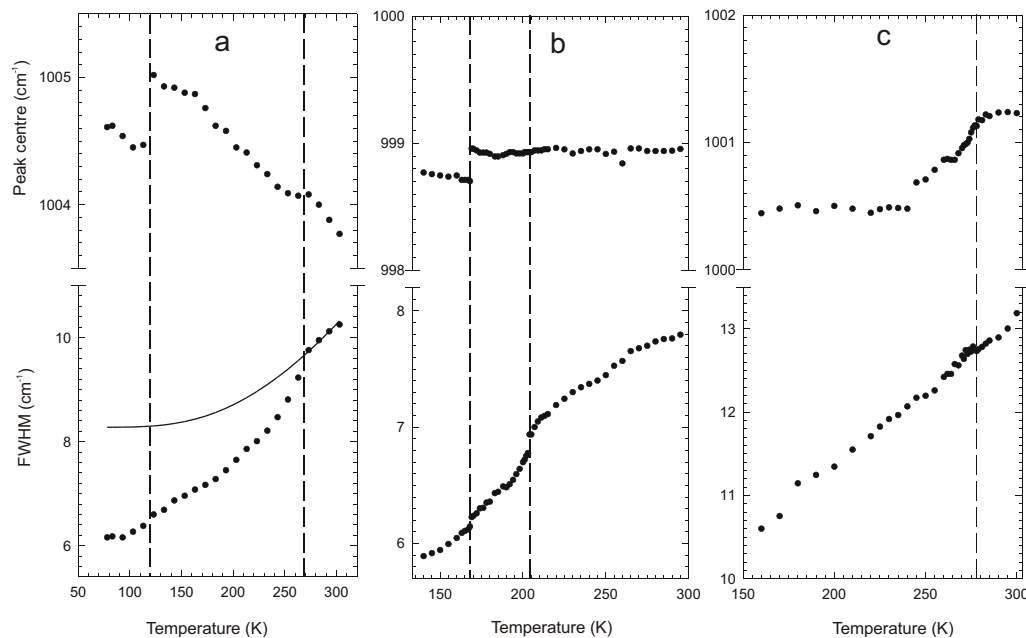

Fig. 3. Full Width Half Maximum and peak centre of the ν_1 sulphate modes in Raman spectra as a function of temperature in **(a)** leonite, **(b)** "Mn-leonite", and **(c)** mereiterite. Vertical dashed lines indicate the transition temperatures of the $C2/m \leftrightarrow I2/a \leftrightarrow P2_1/a$ phase transitions for leonite and "Mn-leonite", and the transition temperatures of the $C2/m \leftrightarrow P2_1/a$ phase transition for mereiterite. The baseline (solid line) to determine the excess FWHM of the ν_1 mode in leonite (*cf.* Fig. 9) was fitted using the saturation function.

of the ν_4 and ν_3 modes of leonite, "Mn-leonite", and mereiterite are presented in Fig. 2.

The $I2/a \leftrightarrow P2_1/a$ first order phase transitions of the Mg- and Mn-endmembers (Hertweck *et al.*, 2001) are characterised by the sudden appearance of additional sulphate stretch-

ing and bending modes. In the Raman spectrum of leonite at 113 K additional bands appear at 1145, 1100, 1090, and 630 cm^{-1}, which are not observed in the spectra above 113 K (Fig. 2a). A stretching band at 1095 cm^{-1}, which is visible in the spectra recorded above 113 K, suddenly disappears at
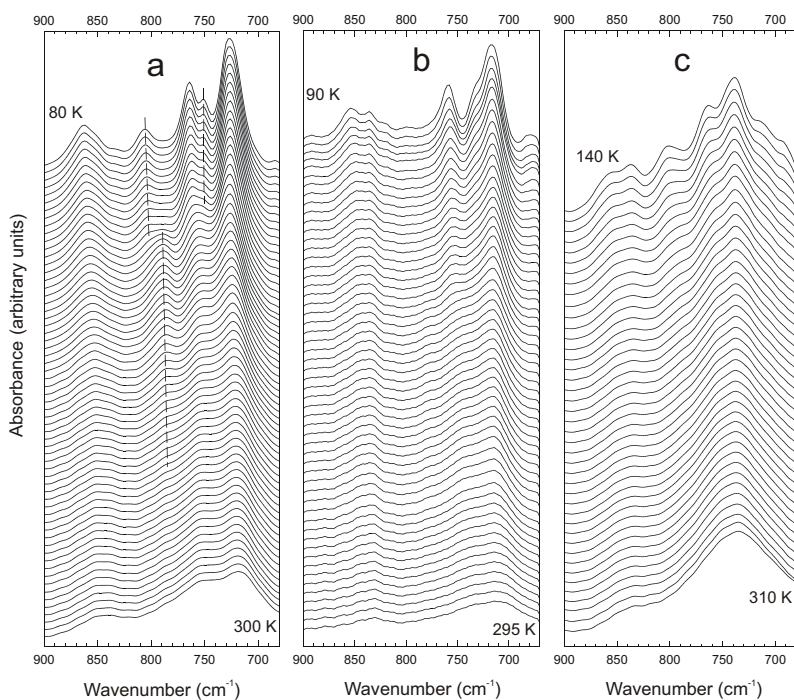
Fig. 4. FTIR absorption spectra of the sulphate bending modes of the leonite-type compounds in the indicated temperature ranges. Dashed lines (as a guide for the eye) indicate the appearance and disappearance of vibrational modes at the $I2/a \leftrightarrow P2_1/a$ phase transitions in leonite. **(a)** Spectra of leonite are measured in temperature steps of 5 K (300–280 K), of 2 K (280–276 K), of 1 K (276–264 K), of 2 K (264–250 K), of 5 K (250–130 K), of 2 K (130–120 K), and of 5 K (120–80 K). **(b)** Spectra of "Mn-leonite" are measured in temperature steps of 5 K (295–215 K), of 2 K (212–206 K), of 1 K (206–198 K), of 2 K (198–190 K), of 5 K (190–180 K), of 2 K (177–173 K), of 1 K (173–170 K), of 2 K (170–168 K), of 5 K (165–120 K), and of 10 K (120–90 K). **(c)** Spectra of mereiterite are measured in temperature steps of 5 K (310–285 K), of 2 K (285–279 K), of 1 K (279–272 K), of 2 K (272–250 K), of 5 K (250–210 K), and of 10 K (210–140 K). Spectra are displayed with an offset of 0.03 in absorbance units.

the $I2/a \leftrightarrow P2_1/a$ phase transition, *i.e.*, it can not be observed in the temperature range below 123 K. For "Mn-leonite" additional bands at 1145, 1120, 1105, 1095, and 1080 cm^{-1} appear in the spectrum at 168 K, which are not visible in the spectra recorded above 168 K (Fig. 2b). Two strong stretching bands of "Mn-leonite" at 1105 and 1085 cm^{-1} suddenly disappear at the $I2/a \leftrightarrow P2_1/a$ phase transition. In addition, discontinuities at the phase transition temperature occur in the ~1105 cm^{-1} band position of leonite and in the ~625 cm^{-1} band position of "Mn-leonite", which otherwise show continuous peak shifts to lower frequencies during cooling.

Fitting of the peak positions of the intense symmetric ν_1 sulphate stretching mode in the Raman spectra of leonite and "Mn-leonite" reveals a discontinuity at the $I2/a \leftrightarrow P2_1/a$ phase transition (Fig. 3). The peak position of the ν_1 vibrational mode in leonite jumps from 1005.0 cm^{-1} at 123 K to 1004.5 cm^{-1} at 113 K, which is a discontinuity in the continuous peak shift below and above the transition temperature of 120 K (Hertweck *et al.*, 2002). In "Mn-leonite" the peak position of the ν_1 vibrational mode as a function of the temperature is constant below and above the $I2/a \leftrightarrow P2_1/a$ phase transition, but shows a discontinuity between 169 and 168 K, jumping from 999 to 998.7 cm^{-1}, which represents exactly the phase transition temperature indicated by optical and calorimetric data (Hertweck *et al.*, 2002). The FWHMs of the ν_1 vibrational modes are almost unaffected by the $I2/a \leftrightarrow P2_1/a$ phase transition (Fig. 3a-b).

The $C2/m \leftrightarrow I2/a$ order-disorder phase transition of leonite and "Mn-leonite" (Hertweck *et al.*, 2001) proceeds continuously. It is not clearly visible in the ν_3 and ν_4 tetrahedral modes (Fig. 2a-b), but is indicated by the position and FWHM of the strong ν_1 vibrational mode as a function of temperature (Fig. 3a-b). During cooling of leonite, the linear increase of the ν_1 band position as well as the linear decrease of the FWHM change non-linearly at 268 K. The order-disorder phase tran-

sition in "Mn-leonite" at 205 K occurs also as a non-linear shift of the FWHM of the ν_1 mode, whereas the band position is not affected by the ordering process at all.

The $C2/m \leftrightarrow P2_1/a$ order-disorder phase transition of mereiterite (Hertweck *et al.* 2001) proceeds continuosly. It is not clearly visible in the ν_3 ν_4 tetrahedral modes (Fig. 2c), but is indicated by the position and FWHM of the strong ν_1 vibrational mode as a function of temperature (Fig. 3c), but shows a contrasting behaviour to leonite and "Mn-leonite". Whereas the decrease of the FWHM is nearly unaffected by the phase transition at 277 K, the shift of the band position with decreasing temperature changes significantly. Within the stability range of the $C2/m$ phase the ν_1 band position remains constantly at ~1001.2 cm^{-1}. Close to the $C2/m \leftrightarrow P2_1/a$ phase transition temperature the band position starts to shift linearly towards lower frequencies. At ~243 K the shift of the band position is interrupted at ~1000.6 cm^{-1}, 35 K below the phase transition temperature, by a discontinuity which can be possibly attributed to the errors and the step width of the measurements. Upon further cooling the band position remains nearly constant, comparable to the band position below the $I2/a \leftrightarrow P2_1/a$ phase transition of "Mn-leonite". This peculiar protracted reaction at the $C2/m \leftrightarrow P2_1/a$ transition of mereiterite is also observed in IR absorption spectra (see below) and X-ray diffraction.

FTIR absorption spectroscopy

Unpolarised FTIR absorption spectra of the three leonite-type compounds are presented in Fig. 4 for the sulphate bending modes from 680 to 900 cm^{-1}, in Fig. 5 for the sulphate stretching modes from 980 to 1230 cm^{-1}, and in Fig. 6 for the O–H stretching modes from 2940 to 3600 cm^{-1}.

Similar to the Raman studies, the $I2/a \leftrightarrow P2_1/a$ first order phase transition of the Mg- and Mn-endmembers (Hertweck
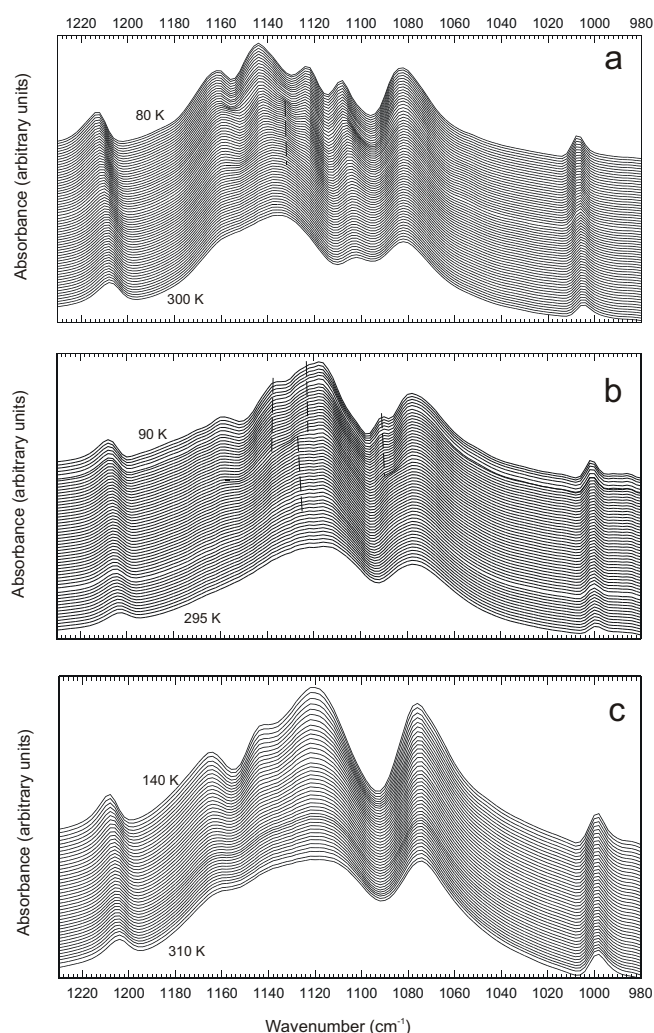
Fig. 5. FTIR absorption spectra of the sulphate stretching modes in **(a)** leonite, **(b)** "Mn-leonite", and **(c)** mereiterite. Dashed lines indicate the appearance and disappearance of vibrational modes at the $I2/a \leftrightarrow P2_1/a$ phase transitions in leonite and "Mn-leonite". Temperature steps of the measurements and offset of the spectra as in Fig. 4.

et al., 2001) is characterised by the sudden appearance of additional sulphate stretching and bending modes. In the FTIR absorption spectrum of leonite at 130 K additional bending modes appear at 805 and 750 cm⁻¹, that can not be observed in the spectra recorded in the temperature range above 130 K. Vibrational modes at 1133 and 790 cm⁻¹, which are visible in the spectra recorded above 130 K, suddenly disappear at the $I2/a \leftrightarrow P2_1/a$ phase transition. For "Mn-leonite" additional stretching bands at 1138 and 1090 cm⁻¹ appear in the spectrum at 180 K, that are not visible in the spectra recorded at temperatures above 180 K. A stretching band of "Mn-leonite" at 1126 cm⁻¹ suddenly disappears at the $I2/a \leftrightarrow P2_1/a$ phase transition.

In addition, in the range of the O–H stretching modes the $I2/a \leftrightarrow P2_1/a$ phase transition of the leonite and "Mn-leonite" is indicated. Although FTIR absorption measurements of the O–H stretching modes result in a broad unresolvable band at room temperature, single peaks are resolved at low temperatures. In leonite the $I2/a \leftrightarrow P2_1/a$ phase transition is

indicated by the sudden appearance of a stretching mode at 3190 cm⁻¹, whereas in "Mn-leonite" the corresponding peak appears at 3170 cm⁻¹. In general, the wide range of O–H stretching frequencies is in good correlation (Libowitzky, 1999) to the wide range of O–H⋯O distances from 2.65 to 2.81 Å (Hertweck *et al.*, 2001).

The transition temperatures of 130 and 180 K indicated by the FTIR absorption spectra for the $I2/a \leftrightarrow P2_1/a$ phase transitions in leonite and "Mn-leonite", respectively, correspond neither with the temperatures indicated by the Raman spectroscopy measurements nor with optical, calorimetric, and X-ray diffraction measurements (Hertweck *et al.*, 2002). This temperature discrepancy of about 10 K may originate from the preparation method. The KBr and the sample powder are compacted with a pressure of 1 GPa, of which a residual strain may remain within the pellet and thereby raise the transition temperature at the low-temperature transition. Another reason may be the small grain size of the milled sample, thus reducing the strain barriers during a ferroelastic transition and facilitating an earlier transition.

In contrast to the Raman spectra, in which at least the position of the strong single ν_1 mode is clearly visible, in the FTIR absorption spectra of leonite and "Mn-leonite" the peak shifts of single sulphate and O–H modes are difficult to pursue. Despite the complex spectra with multiple overlapping peaks, the discontinuities, characterising generally the $I2/a \leftrightarrow P2_1/a$ phase transition (Hertweck *et al.*, 2002), can be detected on some isolated peaks. However, the $C2/m \leftrightarrow I2/a$ order-disorder phase transition of leonite and "Mn-leonite", generally occurring as non-linear changes of optical, calorimetric and X-ray data (Hertweck *et al.*, 2002), is almost undetectable by means of band positions of the SO_4 and O–H vibrational modes as a function of temperature.

Nevertheless, the $C2/m \leftrightarrow P2_1/a$ order-disorder transition of mereiterite (Hertweck *et al.*, 2001) is clearly indicated by the position of the vibrational modes as a function of temperature (Fig. 7). The temperature-dependent shift of the band positions changes significantly at the $C2/m \leftrightarrow P2_1/a$ phase transition temperature at 277 K for the bands at 1160, 1122, 1075, 999, and 738 cm⁻¹. For all these modes another change (and minimum) of the peak shift is observed about 20 K below the phase transition. This peculiar behaviour at the $C2/m \leftrightarrow P2_1/a$ transition of mereiterite is also indicated by Raman spectra (as described above) and X-ray diffraction (Hertweck *et al.*, 2002). Especially the peak shift of the 738 cm⁻¹ mode (Fig. 7a) resembles the behaviour of the *a* lattice parameter. As indicated by two independent X-ray diffraction measurements, the *a* lattice parameter in the $P2_1/a$ phase of mereiterite also shows a further decrease, reaching a minimum ~25 K below the transition temperature (Fig. 7b).

Autocorrelation analysis

To obtain insights into their thermodynamic behaviour, order-disorder phase transitions may be conveniently characterised by changes of the line widths in the Raman and IR spectra, which scale with the Landau order parameter Q (Salje, 1992; Salje & Bismayer, 1997; Salje *et al.*, 2000).
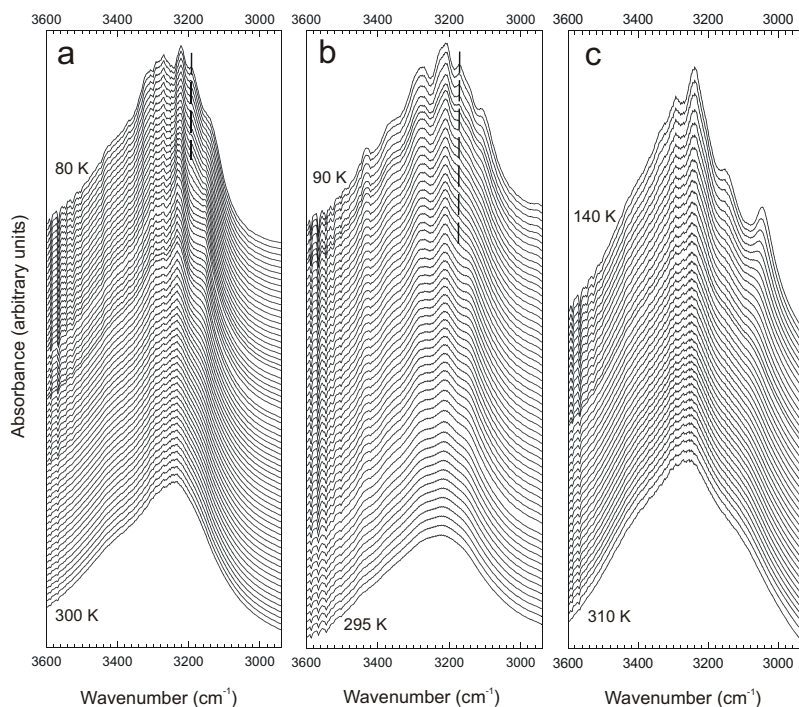
Fig. 6. FTIR absorption spectra of the O–H stretching modes in **(a)** leonite, **(b)** "Mn-leonite", and **(c)** mereiterite. Dashed lines indicate the appearance of additional vibrational modes at the $I2/a \leftrightarrow P2_1/a$ phase transitions in leonite and "Mn-leonite". Temperature steps of the measurements and offset of the spectra as in Fig. 4.
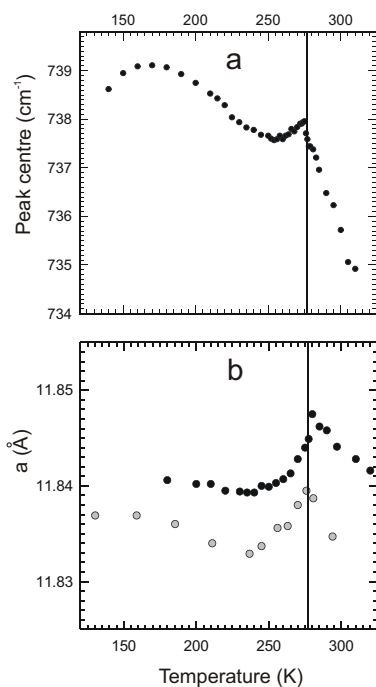

Fig. 7. **(a)** Peak centre of an infrared SO_4 bending mode of mereiterite at ~738 cm^{-1} and **(b)** a lattice parameter of mereiterite as a function of temperature (Hertweck *et al.*, 2002). Vertical lines indicate the transition temperature of the $C2/m \leftrightarrow P2_1/a$ phase transition for mereiterite at 277 K. Data collection of the lattice parameters was done on one crystal on a CAD4 single-crystal diffractometer (grey data points) and on a CCD diffractometer (black data points). Errors in a lattice parameter are within the size of the plotted data points.

Thus, extraction of reliable FWHMs from these spectra is required. Unfortunately, the leonite-type compounds give complex Raman and IR absorption spectra with multiple overlapping peaks. Fitting of single peaks to determine their line widths becomes impossible, aggravated by the difficulty to decide on the number of modes contributing to an individual group of peaks. Salje *et al.* (2000) review the method of autocorrelation analysis as a versatile tool for characterising band widths in phonon spectra with even the most complex band shape.

Salje *et al.* (2000) emphasise that the autocorrelation analysis does not require formal assignment or deconvolution of observed bands to their particular phonon modes. This is an advantage, if we consider that the leonite-type spectra were measured unpolarised and the preparation of single-crystal samples was impossible. A second advantage is the effectiveness of the method when small incremental changes between the collected spectra at different temperatures are of interest, like the changes in the spectra at the order-disorder phase transitions of leonite, "Mn-leonite" ($C2/m \leftrightarrow I2/a$), and mereiterite ($C2/m \leftrightarrow P2_1/a$). A third advantage is that the noise from the spectra is averaged by integration over a broad spectral segment.

The procedure of the autocorrelation analysis (Salje *et al.*, 2000) starts with the selection of an appropriate segment of the primary Raman or IR spectra, which contain some information on the changes during a phase transition. Then, a suitable linear baseline between the end points is subtracted from this segment in each spectrum that was measured at a certain incrementing temperature. Each segment is correlated with itself using the autocorrelation function Corr(α,ω') $= \int \alpha(\omega + \omega') \, \alpha(\omega) \, d\omega$ (Salje *et al.*, 2000) to produce an autocorrelated spectrum at each temperature of the primary spectra. $\alpha(\omega)$ is the absorbance (IR) or intensity (Raman) of the spectrum at a certain frequency ω and $\alpha(\omega + \omega')$ is the same spectrum offset in frequency by ω'.

The width of the central peak of the autocorrelated spectrum varies with the general width of the peaks in the prima-
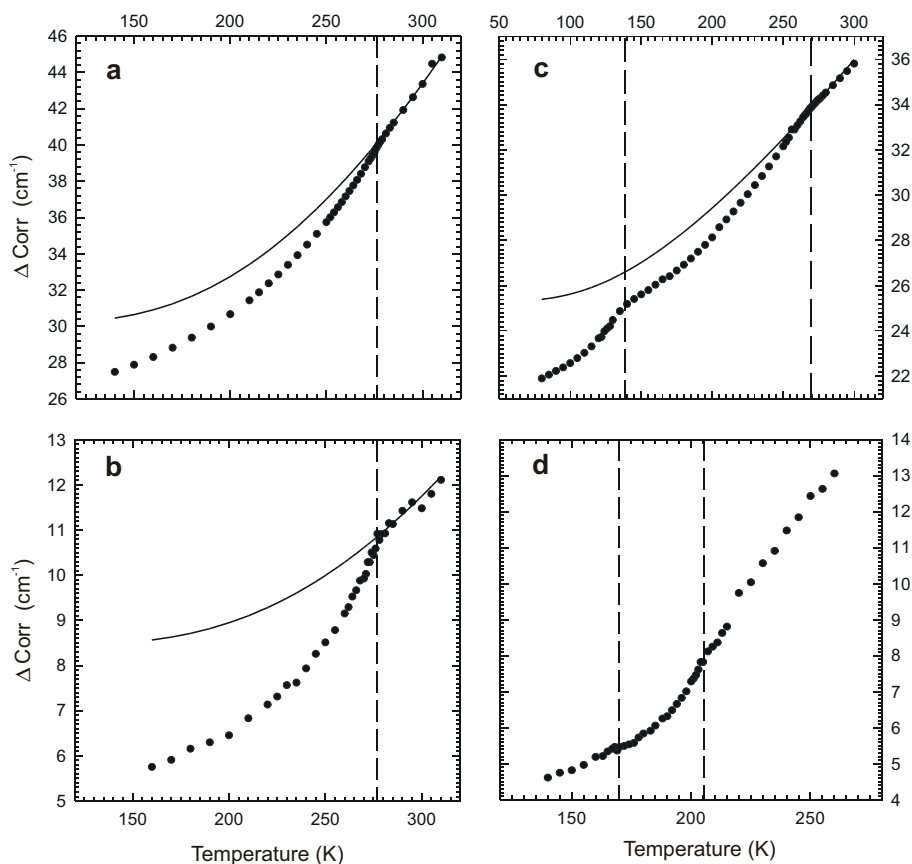
Fig. 8. Examples of autocorrelation analyses of Raman and FTIR absorption spectra of leonite-type compounds. Vertical dashed lines indicate the transition temperatures of the $C2/m \leftrightarrow I2/a \leftrightarrow P2_1/a$ phase transitions for leonite and "Mn-leonite", and the transition temperature of the $C2/m \leftrightarrow P2_1/a$ phase transition for mereiterite. Variation of Δ Corr is plotted as a function of temperature calculated from **(a)** IR spectra of mereiterite in the range between 900 and 1300 cm^{-1}, **(b)** Raman spectra of mereiterite in the range between 1095.3 and 1159.8 cm^{-1} shift, **(c)** IR spectra of leonite in the range between 900 and 1300 cm^{-1}, **(d)** Raman spectra of "Mn-leonite" in the range between 1053.3 and 1153.2 cm^{-1} shift. Baselines (solid lines) to determine δ ΔCorr (*cf.* Fig. 9) were fitted using the saturation function.

ry spectrum, thus containing the combined information of line widths of a complex sequence of peaks. Quantitative information on the primary line widths is extracted by extrapolation of the line width of the central peak of the autocorrelated spectrum in the limit of $\omega' \rightarrow 0$ (Salje *et al.*, 2000). Therefore a Gaussian curve is fitted to the central peak around the offset $\omega' = 0$ for successive ranges of ω' between $2 – 10$ cm^{-1} (IR) and $1.6 – 8.1$ cm^{-1} (Raman) for the autocorrelated spectra. The value of the FWHM of the Gaussian curve at $\omega' = 0$, termed Δ Corr [cm^{-1}], is obtained by extrapolation using a second order polynomial.

The autocorrelation analysis has been applied to several segments in the Raman and IR absorption spectra of the three leonite-type compounds. Four examples of autocorrelation analyses are given in Fig. 8 representing the changes at the order-disorder phase transitions of leonite, "Mn-leonite" ($C2/m \leftrightarrow I2/a$), and mereiterite ($C2/m \leftrightarrow P2_1/a$).

In the IR absorption spectra of mereiterite a segment in the range of the ν_3 sulphate stretching modes between 900 and 1300 cm^{-1} is chosen for autocorrelation analysis (Fig. 8a). The Δ Corr values decrease linearly with decreasing temperature towards the $C2/m \leftrightarrow P2_1/a$ phase transition point at 277 K. At the transition point the slope increases discontinuously. Upon further cooling the Δ Corr values continue with a non-linear decrease. The Δ Corr curve of the Raman spectra of mereiterite is similar (Fig. 8b), with the segment for autocorrelation also chosen in the range of the ν_3 stretching modes between 1095.3 and 1159.8 cm^{-1}. The increase of the slope at the phase transition point is

stronger. In general, the Δ Corr curves autocorrelated from Raman data are more noisy. The narrow peak shapes in Raman spectra compared to the IR spectra result in sharper autocorrelated peaks, implying larger relative errors for the Gauss fits.

In the range of the order-disorder phase transition the appearance of the Δ Corr curve for the IR sulphate ν_3 stretching modes in leonite (Fig. 8c) is similar to the Δ Corr curves of mereiterite, calculated from both IR and Raman spectra (Fig. 8a-b). A segment between 900 and 1300 cm^{-1} has been chosen for autocorrelation analysis.

The curve of Δ Corr values of "Mn-leonite" (Fig. 8d), calculated from Raman spectra in the range of the sulphate ν_3 stretching modes between 1053.3 and 1153.2 cm^{-1}, appears similar to the curve of leonite (Fig. 8c) over the whole temperature range of the $C2/m \leftrightarrow I2/a \leftrightarrow P2_1/a$ phase transitions. However, because of numerous outliers and noise above 205 K, these data were not included in further calculations (see below).

The thermodynamic interpretation of the order-disorder phase transition, which is common to all three leonite-type compounds, needs a quantification of the changes of the Δ Corr values. Determination of the excess Δ Corr values requires the choice of a baseline, which is obtained in this case by fits of the equation $y = a + b \cdot \coth (\theta_s/T)$ to the experimental data in the range of the $C2/m \leftrightarrow I2/a$ ($P2_1/a$ in mereiterite) phase transition (Fig. 8). This baseline function, which describes the change in slope at low temperatures due to normal saturation effects (θ_s = sat. temp.), was also used
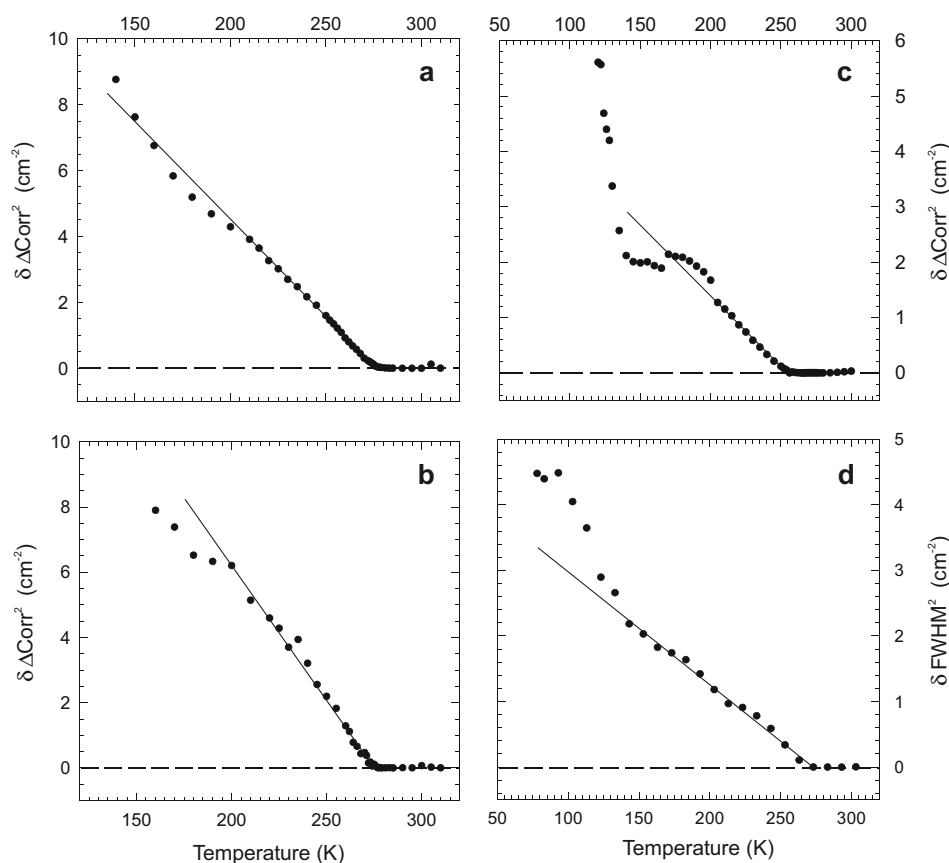
Fig. 9. The thermal evolution of $(\delta\Delta\mathrm{Corr})^2$ and $(\delta\mathrm{FWHM})^2$ for **(a)** autocorrelated IR spectra of mereiterite in the range between 900 and 1300 cm^{-1}, **(b)** autocorrelated Raman spectra of mereiterite in the range between 1095.3 and 1159.8 cm^{-1} shift, **(c)** autocorrelated IR spectra of leonite in the range between 900 and 1300 cm^{-1}, **(d)** ν_1 Raman stretching mode of leonite. Errors in the order parameters are within the size of the plotted data points.

by Salje *et al.* (1991). The values of excess Δ Corr (δ Δ Corr) are determined as the difference between the measured Δ Corr and the baseline. Taking into account pre-transitional effects at the order-disorder phase transition (indicated by a slight deviation from the linear behaviour closely above T_c) only data points ~15 K above the phase transition temperature are used for the baseline fit. Similar and more pronounced pre-transitional effects were observed, *e.g.*, in lawsonite (Sondergeld *et al.*, 2000).

Landau theory

Free energy changes characterise the nature of structural phase transitions. For the phase transitions of leonite-type compounds the structural mechanisms involved have already been revealed by single-crystal structure analysis (Hertweck *et al.*, 2001). The changes in the atomic interactions are expressed in changes of macroscopic properties such as optical birefringence, volume, thermal properties (Hertweck *et al.*, 2002) or vibrational modes. These macroscopic properties can be measured and related to a thermodynamic classification.

The distortion of the structure as a function of temperature, mainly due to the rotation of the sulphate groups in the leonite-type compounds, leads to slight changes of the forces within and surrounding the rigid units. These may be related to variations of the positions and the FWHMs of Raman and IR absorption bands in the range of the sulphate

and O–H vibrational modes. The line width and frequency of every absorption band, with exception of the soft mode, is expected to vary with the squared Landau order parameter Q^2 (Carpenter, 1992; Salje, 1992; Salje & Bismayer, 1997; Salje *et al.*, 2000). However, the magnitude of this variations varies between different absorption bands. Because autocorrelation (Salje *et al.*, 2000) gives a weighted average of the line widths of the bands in the range over which the analysis is made, Δ Corr values are also expected to scale with Q^2.

The $C2/m \leftrightarrow I2/a$ (leonite, "Mn-leonite") and $C2/m \leftrightarrow P2_1/a$ (mereiterite) order-disorder transitions proceed continuously, as indicated by the kind of change of the positions and the FWHMs of several Raman and IR absorption modes (Fig. 1-6). In contrast, the displacive $I2/a \leftrightarrow P2_1/a$ phase transitions of leonite and "Mn-leonite" are characterised mainly by discontinuities in positions and FWHMs of vibrational modes at the transition temperatures. These discontinuities are in agreement with discontinuities in cell volume, intensities of X-ray reflections, as well as optical and calorimetric data (Hertweck *et al.*, 2002), indicating a first order phase transition for $I2/a \leftrightarrow P2_1/a$, thermodynamically characterised by a jump of the order parameter Q from $Q = 0$ to $Q > 0$ at the transition temperature T_c.

The excess free energy due to a phase transition can be described as a polynomial expansion of the order parameter Q (Landau & Lifshitz, 1980; Tolédano & Tolédano, 1987). By minimising the free energy G with respect to Q the equilibrium behaviour through the phase transition is deter-

mined as $dG/dQ = a(T - T_c)Q + BQ^3 + cQ^5$. With $B = 0$ two terms of the free energy expansion are sufficient to describe the free energy changes of the $C2/m \leftrightarrow I2/a$ (leonite, "Mn-leonite") and $C2/m \leftrightarrow P2_1/a$ (mereiterite) order-disorder transitions using the excess Δ Corr, calculated from the experimental data of the line width of several Raman and IR absorption modes. The excess Δ Corr correspond to the squared order parameter Q (Salje, 1992; Salje & Bismayer, 1997; Salje *et al.*, 2000), of which the equilibrium variation with temperature is $Q = a/c (T_c - T)^\beta$. The critical exponent β is ½ for a 2nd order, and ¼ for an ideal tricritical transition (Carpenter, 1992). Thus, the tricritical transition ($B = 0$) represents the boundary between the first order ($B < 0$) and the second order transition ($B > 0$).

The plots of $(\delta\Delta$ Corr$)^2$ *versus* temperature in Fig. 9 are close to linear for the $C2/m \leftrightarrow P2_1/a$ transition of mereiterite (Fig. 9a-b) and for the $C2/m \leftrightarrow I2/a$ transition of leonite (Fig. 9c), implying tricritical behaviour of these order-disorder phase transitions ($Q^4 \propto |T_c - T|$). Fitting of the experimental data of $\delta\Delta$ Corr results in a critical exponent β of 0.25 for the Raman and IR spectra of mereiterite as well as for the IR spectra of leonite. In addition, the variation of the order parameter calculated from primary data (FWHM of ν_1 mode in Raman spectra) of leonite (Fig. 3a) is in excellent agreement with the data from autocorrelation analysis (Fig. 9d). These results confirm the tricritical character of the $C2/m \leftrightarrow I2/a$ ($P2_1/a$) order-disorder phase transitions and are in good agreement with the evaluation of the birefringence and X-ray diffraction data (Hertweck *et al.*, 2002), establishing a critical exponent of 0.20 to 0.22.

References

Carpenter, M.A. (1992): Thermodynamics of phase transitions in minerals: a macroscopic approach. *In* Stability of minerals, Price G.D. and Ross N.L. (Eds). Chapman & Hall, London, 368 p.

Hertweck, B., Giester, G., Libowitzky, E. (2001): The crystal structures of the low-temperature phases of leonite-type compounds, $K_2Me(SO_4)_2 \cdot 4H_2O$ (Me = Mg, Mn, Fe). *Am. Mineral.*, **86**, 1282–1292.

Hertweck, B., Armbruster, T., Libowitzky, E. (2002): Multiple phase transitions of leonite-type compounds: optical, calorimetric, and X-ray data. *Mineral. Petrol.*, **75**, 245-259.

Irmer, G. (1985): Zum Einfluß der Apparatefunktion auf die Bestimmung von Streuquerschnitten und Lebensdauern aus optischen Phononenspektren. *Exp. Tech. Phys.*, **33**, 501–506.

Landau, L.D. & Lifshitz, E.M. (1980) Statistical physics, 3rd edition. Pergamon Press, Oxford, 484 p.

Libowitzky, E. (1999): Correlation of O–H stretching frequencies and O–H⋯O hydrogen bond lengths in minerals. *Monatsh. Chem.*, **130**, 1047–1059.

Nakamoto, K. (1997): Infrared and Raman spectra of inorganic and coordination compounds. Part A: Theory and applications in inorganic chemistry, 5th edition. Wiley-Interscience, New York, 408 p.

Nasdala, L. & Massonne, H.-J. (2000): Microdiamonds from the Saxonian Erzgebirge, Germany: In situ micro-Raman characterisation. *Eur. J. Mineral.*, **12**, 495–498.

Salje, E.K.H. (1992): Hard mode spectroscopy: experimental studies of structural phase transitions. *Phase Trans.*, **37**, 83–110.

Salje, E.K.H. & Bismayer, U. (1997): Hard mode spectroscopy: the concept and applications. *Phase Trans.*, **63**, 1–75.

Salje, E.K.H., Wruck, B., Marais, S. (1991): Order parameter saturation at low temperatures – numerical results for displacive and o/d systems. *Ferroelectrics*, **124**, 185–188.

Salje, E.K.H., Carpenter, M.A., Malcherek, T., Boffa Ballaran, T. (2000): Autocorrelation analysis of infrared spectra from minerals. *Eur. J. Mineral.*, **12**, 503–519.

Schneider, W. (1961): Neubestimmung der Kristallstruktur des Mangan-Leonits, $K_2Mn(SO_4)_2 \cdot 4H_2O$. *Acta Cryst.*, **14**, 784–791.

Srikanta, S., Sequeira, A., Chidambaram, R. (1968): Neutron diffraction study of the space group and structure of manganese-leonite, $K_2Mn(SO_4)_2 \cdot 4H_2O$. *Acta Cryst.*, **B24**, 1176–1182.

Sondergeld, P., Schranz, W., Kityk, A.V., Carpenter, M.A., Libowitzky, E. (2000): Ordering behaviour of the mineral lawsonite. *Phase Trans.*, **71**, 189–203.

Tolédano, J.-C. & Tolédano, P. (1987): The Landau theory of phase transitions. World Scientific, Singapore, 451 p.

Verma, P., Abbi, S.C., Jain, K.P. (1995): Raman scattering probe of anharmonic effects in GaAs. *Phys. Rev.*, **B51**, 16660–16667.